Available online www.jocpr.com

Journal of Chemical and Pharmaceutical Research, 2015, 7(11):99-104

Research Article

ISSN : 0975-7384
CODEN(USA) : JCPRC5

Wet chemical synthesis of magnesium zinc ferrite nanoparticles

Vikas J. Pissurlekar

Department of Chemistry, PES's RSN College of Arts & Science Farmagudi Ponda, Goa, India

---

ABSTRACT

Cubic spinel ferrites are one of the most sought after materials, which have attracted interest in many fields. They are the subject of extensive research owing to their wide range of applications in areas like hyperthermia, information storage systems, gas sensors, microwave devices, magnetic recording media, humidity sensors, etc. Magnesium ferrite, zinc ferrite and the solid solutions between these two ferrites crystallize into cubic spinel structure and have several important technological applications. In this study synthesis of soft magnetic spinel Mg-Zn ferrite(Mg_xZn_{1-x} Fe_2O_4, where x= 0.2, 0.4, 0.6, and 0.8) nanoparticles was carried out using the precursor method. Structural and magnetic properties have been studied in detail. XRD data revealed that the structure of these nanoparticles is spinel and crystallite size are in the range 20-44 nm. Lattice parameter decreases with increasing Mg concentration due to the smaller ionic radius of the Mg^{2+} ion. FTIR spectroscopy also confirmed the formation of spinel ferrite by showing the characteristic absorption bands in the range of 405–396 cm^{-1} and 566–555 cm^{-1}. The magnetization showed an increasing trend with increasing Mg concentration up to x =0.6, due to the rearrangement of cations at tetrahedral and octahedral sites, while the coercivity remained small. It is observed that both structural as well as magnetic properties of Mg-Zn ferrite nanoparticles strongly depend upon Mg^{2+} concentration.

Keywords: Nanoparticles, Magnetic, Lattice parameter, Cations, Coercivity

---

INTRODUCTION

Mixed spinel ferrites have been studied exhaustively over the last few years due to their wide ranging applications [1–4]. Spinel ferrites have the chemical formula MFe_2O_4 in which M can be any divalent metal ion or a mixture of metal ions having average valence of two. The unit cell is cubic. The oxygen ions form a nearly close-packed face centered cubic structure and the metal ions in the unit cell occupy the interstitial positions with four fold and six fold oxygen coordination. The metal ion surrounded by four oxygen ions is called A site which is tetrahedral and that surrounded by six oxygen is called B site which is octahedral. There are 96 interstitial positions with 64 A sites and 32 B sites. However 8 cations occupy A sites and 16 occupy B sites. The occupation of position of metal ions over two sites depends upon the relative site preference and energies of cations present. This governs the intrinsic properties of ferrites.

Depending upon modes of occupation of A and B sites by metal ions and on the basis of cation distribution Barth and Posnjak [5] have classified spinel into three classes as: Normal ferrites, Inverse ferrites and Random or Mixed ferrites.

In normal ferrites all divalent metal ions occupy A sites and all the Fe^{3+} occupy B sites- $Me^{2+}[Fe_2^{3+}]O_4$. Ferrites like $ZnFe_2O_4$, $CdFe_2O_4$ etc are normal ferrites and they are non-magnetic in nature. In inverse ferrite all the eight divalent metal ions and half the Fe^{3+} ions occupy B sites while remaining half of Fe^{3+} occupy A sites- $Fe^{3+}[Fe^{3+}Me^{2+}]O_4$. Examples are $MgFe_2O_4$, $NiFe_2O_4$, $CoFe_2O_4$, Fe_3O_4 etc. Physical properties are strongly influenced by the preference of metal ions on these lattice sites [6]. The concentration and types of cations substitution also have effects on the physical properties [7, 8]. The synthesis methods, chemical composition, and annealing temperature

are responsible for the control of structural and magnetic environments of these two lattice sites. Zinc ferrite has normal spinel structure, in which Zn^{2+} cations mainly occupy tetrahedral sites [9]. While magnesium ferrite has an inverse spinel structure with the preference of Mg^{2+} cations mainly on octahedral sites [10,11], Both Zn^{2+} and Mg^{2+} divalent ions are non-magnetic in nature. An attempt was made to see the influence of the doping of magnesium cation in the zinc ferrite and study its effect on structural and magnetic properties of zinc ferrite nanoparticles.

EXPERIMENTAL SECTION

Mg-Zn ferrite (Mg_xZn_{1-x} Fe_2O_4, where x= 0.2, 0.4, 0.6, and 0.8) nanoparticles were synthesized using a precursor method. The chemical used in this synthesis were magnesium nitrate Mg $(NO_3)_2$ $6H_2O$, zinc nitrate Zn $(NO_3)_2$ $6H_2O$ and ferric nitrate $Fe(NO_3)_3$ $9H_2O$. All the chemicals were of analytical grade. Stoichiometric amount of $Mg(NO_3)_2$ $6H_2O$, $Zn(NO_3)_2$ $6H_2O$ and $Fe(NO_3)_3$ $9H_2O$ were dissolved in minimum quantity of deionized water under constant stirring, to obtain a clear solution. To this solution calculated amount of hydrazinium acetate ligand solution was added slowly with constant stirring and it was thoroughly mixed. The mixture was then kept for drying on a hot plate. The mixture dried to a solid mass which auto-catalytically got decomposed into the powder form and these powders were used for characterization and study of structural, electrical and magnetic properties.

The structural characterization of the prepared Mg-Zn ferrite nanoparticles was carried out using Rigaku, X-ray advance Power diffractometer using Cu Kα radiation (λ = 1·54183 Å). The step size employed was 0·02°, in the range of 20^0–80^0. Infrared Spectroscopy (IR) is one of the versatile tools for both qualitative and quantitative analysis of molecular species. It is employed with the intensity measurements for chemical and structural identification, and for the quantitative measurements. A chemical substance shows a marked selective absorption in the infrared region. After absorption of IR radiations, the (bonds) molecules of chemical compounds vibrate with different rates of vibration producing a close packed absorption bands called IR absorption spectrum, In a typical experiment, the solid ferrite sample was finely ground along with the pure and dry KBr, in the ratio 1:10. Fine grinding is required for the sample to be uniformally mixed with KBr. The mixture was then put in a sample holder and placed in the sample chamber of the IR spectrophotometer. The absorption spectrum for the sample was recorded in the wavelength range 1000$cm^{-1}$to 400cm^{-1}. The experiment was repeated for all the samples.

The average particle size T was calculated using most intense peak (311) employing the Scherer formula. The particle size and morphology studies were carried out using Scanning Electron Microscope Model JEOL 5800LV. The saturation magnetization measurements of all the samples were carried out at room temperature using Pulse Field Magnetic Hysteresis Loop Tracer, supplied by Magneta India Model PFMHT-1. Magnetization, coercivity and remanence magnetization were calculated from the hysteresis loops.

RESULTS AND DISCUSSION

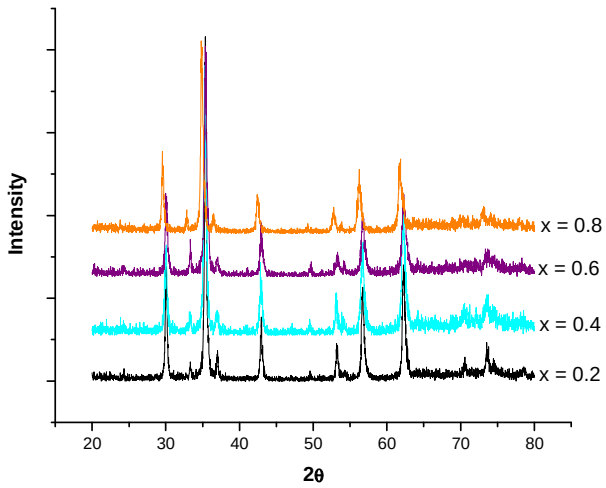

Figure 1: X-ray diffraction patterns of samples Mg_xZn_{1-x} Fe_2O_4

Figure 1 shows the X-ray diffraction patterns of samples Mg_xZn_{1-x} Fe_2O_4, where x= 0.2, 0.4, 0.6, and 0.8 nanoparticles. All the peaks correspond to cubic spinel ferrite structure for all the samples and confirm the formation of single phase ferrite.

Table 1: Variation of lattice constant for various Mg-Zn ferrite samples synthesised

samples	a in cm
$Mg_{0.2}Zn_{0.8}Fe_2O_4$	8.445×10^{-8}
$Mg_{0.4}Zn_{0.6}Fe_2O_4$	8.437×10^{-8}
$Mg_{0.6}Zn_{0.4}Fe_2O_4$	8.411×10^{-8}
$Mg_{0.8}Zn_{0.2}Fe_2O_4$	8.396×10^{-8}

The values for lattice constants were calculated for all $Mg_x Zn_{(1-x)}Fe_2o_4$ nanoparticles using the characteristic (311) peak from XRD pattern. The values of lattice constants are given in Table 1 and plotted as shown in Figure 2. The lattice constant '*a*' is found to decrease with increasing the magnesium content. This decrease in lattice constant with increasing Mg concentration can be attributed to the ionic size differences, where Mg^{2+} ions (0.66Å) are substituted by Zn^{2+}, ions with a larger ionic size (0.82Å) [12]. The lattice parameter 'a' was calculated using lattice spacing (d) values and respective miller indices (hkl) using the formula given in equation 1. The lattice parameters are in the range 8.445 Å -8.396 Å

$$a = d/ (h^2+k^2+l^2)^{½} \quad (1)$$

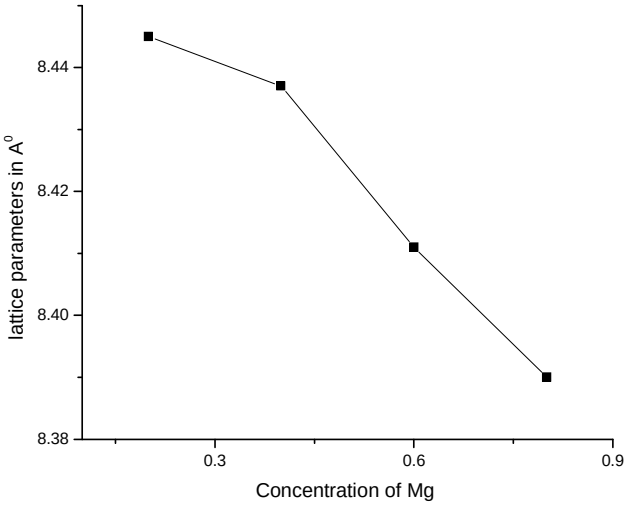

Figure 2 : variation of Lattice Constant with Conc. of Mg

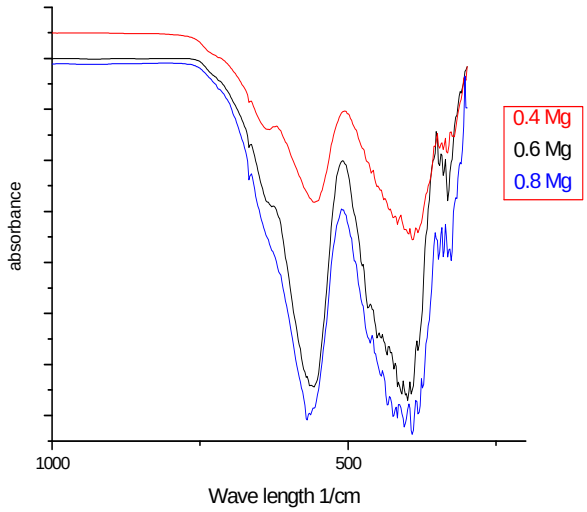

Figure 3: IR spectra of $Mg_xZn_{1-x}Fe_2O_4$samples

Infra red (IR) absorption spectroscopy helps to identify the spinel structure. The three typical vibrational bands associated with spinel structure [13] are at (1) 600-550cm^{-1} (2) 450-385 cm^{-1} (3) 350-330cm^{-1} for metal-oxygen

band. Fourier transformed infra red (FTIR) spectroscopy studies of the nano particle ferrite samples were carried out between 1000 - 400 cm^{-1} as shown in figure 3.

In spinel ferrites, the bands in the ranges of 600–550 cm^{-1} and 450–385 cm^{-1} are assigned to tetrahedral and octahedral metal ions vibrations with oxygen ions, respectively, which are also characteristic bands of spinel ferrite. As can be seen from the figure 3 the presence of two strong absorption bands ν_1 in the range of 566–555 cm^{-1} and ν_2 = 405–396 cm^{-1} for the as prepared samples. The band positions ν_1 and ν_2 are listed in Table 2 as a function of Mg content. The bands ν_1 corresponds to stretching vibration mode due to the vibration of the chemical bond O–$M_{tet.}$–O in location of tetrahedral position and the band ν_2 Corresponds to vibration of the chemical bond O–$M_{oct.}$–O in the metal–oxygen vibration in octahedral sites. The presence of these absorption bands indicates the formation of spinel structure of ferrite samples. It is also observed that the O–$M_{tet.}$–O band is shifted to higher wave numbers with the increase in Mg concentration. It is reported by some researchers [14] that there is a shift in a tetrahedral band of Mg-Zn ferrite towards higher wave number as compared to the Zn ferrite, due to increasing Mg concentration which also gives an indication that preference of Mg ions in occupying tetrahedral lattice sites in addition to octahedral sites. It is quite evident as per the literature available [15] that the Mg^{2+} ions prefer both tetrahedral and octahedral sites in Mg ferrite nanoparticles.

Table 2: Variation of Wavelength.

Composition of Mg	Wavelength cm^{-1}	
	ν_1	ν_2
0.4	555	388
0.6	560	391
0.8	566	396

Average crystallite sizes were calculated by using XRD data by measuring the full-width at half maximum (FWHM) for most intense characteristic (311) peak for each sample with the help of the Scherer formula as given in equation 2, and are in the range 20-44 nm for different Mg concentrations.

$$T=0.9\ \lambda/D_p\cos\theta \qquad (2)$$

Where, T is the average crystallite size, λ is the X-ray wavelength, D_p the angular line width of half maximum intensity and θ is the Bragg angle in degrees. The particle size of $Mg_xZn_{1-x}Fe_2O_4$, where x= 0.2, 0.4, 0.6, and 0.8 nanoparticles with Mg concentration is given in table 3. The crystallite sizes are scattered and in the range 20– 44 nm for different compositions. It is observed that minimum crystallite size of 20 nm is observed for the ferrite sample with Mg concentration of x=0.8 which may be due to the smaller ionic radius of Mg^{2+} ions.

Table 3: Variation of particle size

Samples	Particle size in nm
$Mg_{0.2}Zn_{0.8}Fe_2O_4$	44.1
$Mg_{0.4}Zn_{0.6}Fe_2O_4$	41.9
$Mg_{0.6}Zn_{0.4}Fe_2O_4$	32.8
$Mg_{0.8}Zn_{0.2}Fe_2O_4$	20.5

As can be seen in Figure 4(a), (b) and (c), the microstructure of Mg- Zn ferrites reveal that the nanoparticles are agglomerated due to the presence of magnetic interactions and are of uniform grain size.

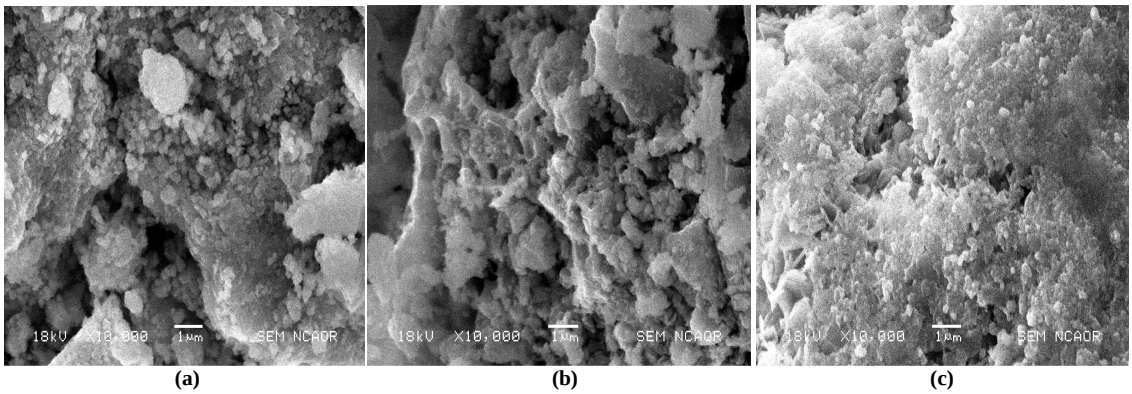

(a) (b) (c)

Figure 4: shows SEM images of $Mg_xZn_{(1-x)}Fe_2o_4$ (x = 0.2,0.6 and 0.8) nanoparticles

Magnetization measurements were carried out at room temperature with a maximum applied magnetic field of 5 kOe. Saturation magnetization is found to increase with increasing Mg concentration till x=0.6 and then decreases for the sample with x=0.8 as shown in Figure 5. The initial increase in saturation magnetization with increasing Mg content can be explained on the basis of Neel's two sub lattice models, which proposes the increase in resultant sub-lattice magnetic moment. Neel [16] considered three types of exchange interaction between unpaired electrons of two ions occupying A and B sites. A–B interaction heavily predominates over A–A and B–B interactions. The A–B interaction aligns all the magnetic spins at A sites in one direction and those at B site in the opposite direction.

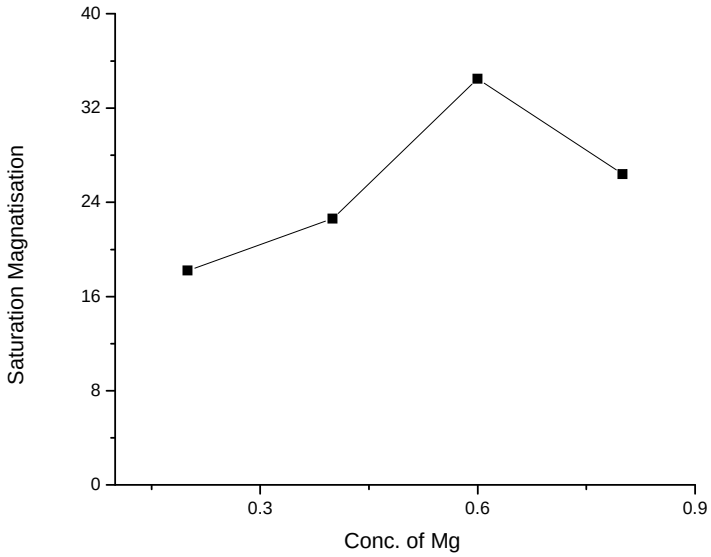

Fig 5: variation of saturation magnetization values of Mg-Zn ferrite

The net moment of the lattice is therefore the difference between the magnetic moments of B and A sub-lattices, i.e., $M = M_B - M_A$. The magnetic moment of each composition depends on the distribution of Fe^{3+} ions between the two sub lattices A and B. The pure bulk Mg ferrite exhibits inverse spinel structure in which Mg^{2+} ions prefer octahedral sites, as it is known that the Mg-ferrite in nanoparticles form is a spinel with certain degree of inversion and shows magnetic behavior due to its incomplete inverse spinel structure at nano-scale [10,11]. The increase of the net magnetization with increasing Mg concentration is due to the distribution of Fe^{3+} ions on octahedral and tetrahedral lattice sites. This distribution of Fe^{3+} ions strengthens the A–B super exchange interactions which results in the increase of the net magnetization [17]. Thus the magnetization of Mg-Zn ferrite nanoparticles depends on the distribution of Fe^{3+} ions among tetrahedral and octahedral lattices sites because both Mg^{2+} and Zn^{2+} ions are non-magnetic in nature.

Table 4: Saturation Magnetization values of Mg-Zn ferrite

Samples	Saturation Magnetization (emu/g)	Coercivity H_c	Retentivity M_r
$Mg_{0.2}Zn_{0.8}Fe_2O_4$	18.2	112.7	1.65
$Mg_{0.4}Zn_{0.6}Fe_2O_4$	22.6	104.9	2.42
$Mg_{0.6}Zn_{0.4}Fe_2O_4$	34.5	119.1	3.64
$Mg_{0.8}Zn_{0.2}Fe_2O_4$	26.4	111.5	2.96

With further increase in nonmagnetic Mg^{2+} ions content, an increasing dilution in A sites takes place, which results to the collinear ferromagnetic phase breaking down at x = 0.6. Further for Mg-Zn ferrite with x=0.8 the triangular spin arrangement on B-sites is suitable and this causes a reduction in A-B interaction and an increase of B-B interaction. Therefore, the decrease of saturation magnetization can be explained on the basis of three sub lattice Yafet-Kittle model [18]. The coercivity (Hc) fluctuates in the range of 100– 120 Oe as the Mg concentration is increased from 0.2 to 0.8. Smaller values of coercivity for all the as prepared samples indicate the soft magnetic nature of these ferrite nanoparticles and also signify the presence of ferromagnetic behavior at room temperature.

CONCLUSION

The present study was carried out to synthesize fine particles Mg-Zn mixed metal ferrite material with formula $Mg_xZn_{1-x}Fe_2O_4$ with x=0.2, 0.4, 0.6, and 0.8 the samples were prepared using a wet chemical method.

Samples were obtained at low temperature and were confirmed by different methods of characterisation such as IR spectral analysis, XRD and SEM analysis.

The lattice constant for the samples are in the range of $8.445A^0$-$8.396A^0$ .The values are in close agreement with the reported values. The average particles size calculated using Scherer formula was in the range of 20nm to 44nm.

Saturation magnetization (Ms) values of samples are found to increase as magnesium content increases, up to Mg content x = 0.6, and decreased for x -0.8 which is attributed to the change in the cationic distribution at tetrahedral and octahedral sites. Smaller values of the coercivity showed the soft magnetic nature of this Mg-Zn mixed metal ferrite.Thus, it can be concluded that the different changes occur in the properties of Mg –Zn ferrite nanoparticles due to the rearrangements of Mg and Zn divalent metal cations at different lattice sites.

REFERENCES

[1] I Sharifi; H Shokrollahi; S Amiri. *J. Magn. Magn.Mater*., **2012**, 324, 903–915.
[2] N Gupta; A Verma; SC Kashyap; DC Dube. *J. Magn. Magn. Mater.*, **2007**, 308,137–142.
[3] M Srivastava; A K Ojha; S Chaubey; A Materny. *J. Alloys and Compounds*, **2009**, 481, 515.
[4] N Gupta; A Verma; SC Kashyap; DC Dube. *J. Magn. Magn. Mater*., **2007**, 308, 137–142.
[5] T FBarth; E Posnjak. Z Krist., **1952**, 82,325.
[6] E Rezlescu; E L Sachelarie; N Rezlescu. *J. Optoelectronics and Advanced Materials*, **2006**, 8, 1019–1022.
[7] M A El Hiti; A I El Shora; SM Hammad. *Mater. Sci. Technol*., **1997**, 13.
[8] T Nakamura; Y. Okano. *J. Phys. IV Fr*., **1997**, 7 (C1), 101.
[9] K P Thummer; MC Chhantbar; KB Modi; GJ Baldha; H H Joshi. *J. Magn. Magn. Mater*., **2004**, 280, 23–30.
[10] J Smit; HPJ Wijn. Ferrites, Wiley, New York, **1959**, p. 143.
[11] Y Ichiyanagi; M Kubota; S Moritake; Y Kanazawa; T Yamada; T Uehashi. *J. Magn. Magn. Mater*., **2007**, 310, 2378.
[12] H Spiers; I P Parkin; Q A Pankhurst; L Affleck; M Green; D J Caruana; M V Kuznetsov; J Yao; G Vaughan; A Terry; A Kvick. *J Mater. Chem*., **2004**, 14, 1104–1111.
[13] R D Waldron. *Phys. Rev*., **1955**, 99, 1727.
[14] S J Keny; J Manjanna; G Venkateswaran; R Kameswaran. *Corrosion Science* **2006**, 48, 2780–2798.
[15] A Pradeep; P Priyadharsini; G Chandrasekaran. *J. Magn. Magn. Mater*., **2008**, 320, 2774.
[16] I Neel. *Ann. Phys*., **1948**, 3, 137.
[17] A Goldman. Modern Ferrite Technology, second ed., Springer, New York, **2006**.
[18] M Ajmal; A Maqsood. *J. Alloy. Comp*., **2008**, 460,54-59.